

Direct-coupling lensing by antisymmetric tensor monopoles

Kamuela N. Lau* and Michael D. Seifert†

Dept. of Physics, Williams College, 33 Lab Campus Dr., Williamstown, MA 01267, USA

We discuss the effects of a direct coupling between a rank-two antisymmetric tensor field and the Maxwell field. The coupling we consider leads to vacuum birefringence, allowing us to place constraints on the magnitude of the tensor field and the strength of its coupling to the Maxwell field via cosmological birefringence measurements. For light propagating in the presence of a topological defect solution, we find that light rays with different polarizations will follow different trajectories; the magnitude of this deflection is predicted to be extremely small (on the order of 10^{-10} arcseconds). We discuss the plausibility of this phenomenon as a method for detection of these monopoles, along with the applicability of our methods to other possible couplings between the tensor field and the Maxwell field.

I. INTRODUCTION

Since its discovery and development at the beginning of the 20th century, Lorentz symmetry has been shown many times to be a very good symmetry of nature. Over the past decade and a half, however, there has been significant interest in investigating the possible ways in which Lorentz symmetry might be violated. One of the more active research programs being pursued to this end is the so-called *Standard Model Extension*, or SME [1]. This program “extends” the Standard Model by relaxing the requirement that the field combinations appearing in the Standard-Model Lagrangian be Lorentz scalars, and allowing combinations that are spacetime tensors to appear in the Lagrangian. Since the total action must still be a scalar, this means that the coefficients of these new terms will also be Lorentz tensors. The presence of these terms in the Lagrangian will affect the equations of motion of the fields (on the classical level) and the field propagators and Feynman rules (on the quantum level); in principle, then, these new tensor coefficients could be measured experimentally.¹ While none of these postulated coefficients have thus far been measured to be unambiguously non-zero, many bounds have been placed on the values of these coefficients, some of which are exceedingly stringent [2].

The SME was initially developed from a particle-physics perspective, and in particular, initially assumed that the “arena” in which fields exist and interact was flat Minkowski spacetime. In the context of flat spacetime, it is legitimate to assume that these new tensor coefficients are constants throughout space and time, and so can be viewed as “constants of nature”. However, it was

soon realized that this simple picture runs into trouble when we try to extend it to curved Riemannian spacetime. The first obvious objection in this case is that while many constant tensor fields exist on a flat manifold (e.g., $\partial_a A^b = 0$ has many solutions), a constant field (e.g., with $\nabla_a A^b = 0$) will not in general exist on a curved manifold. One might try to fix this problem by allowing the tensor coefficients of the new terms to be fixed background tensor fields in the case of curved spacetime. However, this leads us to a second problem with the original conception of the SME, less obvious but more serious. It was shown by Kostelecký [3] that the presence of a fixed background tensor field would necessarily lead to violations of the Bianchi identities. The only way to circumvent this problem, while retaining a spacetime that is well-described by Riemannian geometry, is to allow these “background tensor fields” to be dynamic. Schematically, the full action of the theory will then be of the form

$$S = \int d^4x \sqrt{-g} (-(\nabla\mathcal{T})(\nabla\mathcal{T}) - V(\mathcal{T}) + \mathcal{L}_{\text{SM}}(\Psi) + \mathcal{L}_{\text{LV}}(\Psi, \mathcal{T})), \quad (1)$$

where \mathcal{T} is a “Lorentz-violating” tensor field and Ψ represents the “conventional” matter fields of the Standard Model. In this Lagrangian, \mathcal{L}_{SM} is the Standard Model Lagrangian (including gravity), while \mathcal{L}_{LV} represents a small coupling between conventional matter and the Lorentz-violating tensor field. Since the Lorentz-violating tensor fields will now be dynamic, they will satisfy their own diffeomorphism-invariant equations of motion, and so the Bianchi identities will automatically be satisfied so long as the equations of motion for this field (and the conventional matter fields) hold. By appropriately choosing the form of the potential $V(\mathcal{T})$, we can recover the “original SME” limit of flat spacetime and a constant background tensor field coupled to conventional matter. In such a picture, Lorentz symmetry is broken spontaneously rather than explicitly.

Since the Lorentz-violating tensor field \mathcal{T} must be dynamical, it is natural to ask how this field will behave. The dynamics of such tensor fields in flat spacetime have been widely studied over the past few years, particularly

* Kamuela.N.Lau@williams.edu

† Michael.Seifert@williams.edu

¹ Since these coefficients are tensors, their specification in terms of components is frame-dependent; the standard choice of frame, and the one we will use for this paper, is the “Sun-centered frame”, in which the z -axis is parallel to the axis of Earth’s rotation and the x -axis points towards the Vernal Equinox. Spherical angles in these coordinates are the standard astronomical right ascension and declination.

in the case where \mathcal{T} is a vector field A^a [4–7], a symmetric rank-two tensor field C^{ab} [8], or an antisymmetric rank-two tensor field B_{ab} [9]. Most of this prior work has centered on the situation where the tensor field is constant throughout space, taking on some value $\bar{\mathcal{T}}$ that minimizes its potential energy. However, this field value will not generally speaking be unique. A general potential $V(\mathcal{T})$ which breaks Lorentz symmetry will possess many possible values of \mathcal{T} which minimize the potential energy; these field values form the so-called *vacuum manifold* in field space. This raises the possibility of topological defect solutions in the cases where the vacuum manifold is topologically non-trivial, and it has been shown that in the case of the antisymmetric rank-two tensor field, there exist topological monopole solutions [10, 11]. These solutions are static, stable, and spherically symmetric, but the field is not in the vacuum manifold except asymptotically, and approaches different points in the vacuum manifold as we go to spatial infinity in different directions. Moreover, if an antisymmetric tensor field capable of supporting these defects exists, one would expect a certain number of these monopoles to arise in the early Universe via the Kibble mechanism [12], and these monopoles might persist as relics today. In other words, not only are non-constant tensor fields required in curved spacetimes, but they arise naturally in the context of flat spacetime as well.

The possibility of a stable non-constant background for a Lorentz-violating field leads us to ask what the effects of such a field on matter would be. To the best of our knowledge, all prior work dealing with Lorentz violation (particularly within the SME program [4–9]) has only dealt with position-independent effects; however, the existence of monopole solutions provides us with the motivation that position-dependent effects might be physically relevant. In this paper, we examine the effects of an antisymmetric tensor monopole as a background field coupled to the electromagnetic field. In Section II, we present our model and review the formalism used to examine Lorentz-violating effects in electrodynamics. In Section III, we use polarimetry data to gain an idea of the size of the effects which will arise and bound the parameters of our model. The main results of this work are then derived in Section IV, in which it is shown that an antisymmetric tensor monopole coupled directly to light would cause a lensing effect on light rays, akin to a gravitational lensing effect but in flat spacetime.

We will use units throughout where $\hbar = c = 1$. The metric signature will be $(-, +, +, +)$.

II. LORENTZ-VIOLATING ELECTRODYNAMICS

The main objects of interest in this paper will be a conventional Maxwell field A_a and an antisymmetric rank-

two tensor field B_{ab} . The action for this model is

$$\mathcal{L} = -\frac{1}{4}F_{ab}F^{ab} - \frac{1}{6}F_{abc}F_{abc} - V(B_{ab}) - (k_F)^{abcd}F_{ab}F_{cd}, \quad (2)$$

where $F_{ab} = 2\partial_{[a}A_{b]}$ is the field strength for the Maxwell field; $F_{abc} = 3\partial_{[a}B_{bc]}$ is the field strength for the ‘‘Lorentz-violating’’ field B_{ab} ; $V(B_{ab})$ is a potential energy for B_{ab} , given by

$$V(B_{ab}) = \frac{\lambda}{4}(B_{ab}B^{ab} - b^2)^2; \quad (3)$$

and $(k_F)^{abcd}$ is a tensor that couples the Maxwell field to the Lorentz-violating field, given by²

$$(k_F)^{abcd} = \xi \left(B^{ab}B^{cd} - B^{[ab}B^{cd]} - \frac{1}{6}\eta^{a[c}\eta^{d]b}B_{ef}B^{ef} \right). \quad (4)$$

The tensor $(k_F)^{abcd}$ can be seen to be dimensionless; this implies that the parameter ξ has mass dimension -2 . The parameter ξ is assumed to be a ‘‘small’’ parameter that determines the strength of the coupling; we will assume it to be non-zero, but in principle it could be either positive or negative. The first ‘‘subtraction’’ term in (4) is chosen to eliminate a term proportional to $\epsilon_{abcd}F^{ab}F^{cd}$, which is a total derivative and so would not contribute to the equations of motion. The second subtraction is chosen to eliminate a term proportional to $F_{ab}F^{ab}$, which would simply rescale the factor of $\frac{1}{4}$ in front of the ‘‘Lorentz-invariant’’ kinetic term for the Maxwell field. An arbitrary tensor with these symmetries would have 19 independent components [13]; however, since our $(k_F)^{abcd}$ is constructed out of the antisymmetric tensor B_{ab} , it only has six independent degrees of freedom.

The effects of an arbitrary tensor $(k_F)^{abcd}$ on electromagnetic fields have been formalized by Kostelecký and Mewes [13]. The behaviour of the fields in the presence of such a coupling is equivalent to their behaviour in a linear medium:

$$\begin{aligned} \vec{\nabla} \cdot \vec{D} &= 0, & \vec{\nabla} \times \vec{H} - \frac{\partial \vec{D}}{\partial t} &= 0, \\ \vec{\nabla} \cdot \vec{B} &= 0, & \vec{\nabla} \times \vec{E} + \frac{\partial \vec{B}}{\partial t} &= 0. \end{aligned} \quad (5)$$

The constitutive relations of this ‘‘medium’’ are given by

$$\begin{bmatrix} \vec{D} \\ \vec{H} \end{bmatrix} = \begin{bmatrix} \mathbf{1} + \kappa_{DE} & \kappa_{DB} \\ \kappa_{HE} & \mathbf{1} + \kappa_{HB} \end{bmatrix} \begin{bmatrix} \vec{E} \\ \vec{B} \end{bmatrix}, \quad (6)$$

where $\mathbf{1}$ is the 3×3 identity matrix and the κ 's are 3×3

² This is, of course, not the only possible coupling between B_{ab} and A_a ; see Section V for further discussion.

matrices given by

$$(\kappa_{DE})^{ij} = -2(k_F)^{0i0j}, \quad (7a)$$

$$(\kappa_{DB})^{ij} = -(\kappa_{HE})^{ji} = (k_F)^{0ikl}\epsilon^{jkl}, \text{ and} \quad (7b)$$

$$(\kappa_{HB})^{ij} = \frac{1}{2}\epsilon^{ikl}\epsilon^{jmn}(k_F)^{klmn}. \quad (7c)$$

We define the spatial vectors \vec{Q} and \vec{R} to be the ‘‘electric’’ and ‘‘magnetic’’ parts of B^{ab} , respectively; in other words, $Q^i = B^{0i}$ and $R^i = \frac{1}{2}\epsilon^{ijk}B^{jk}$. In terms of these vectors, we find that

$$(\kappa_{DE})^{ij} = \xi \left[-2Q^i Q^j + \frac{1}{3}(\vec{Q}^2 - \vec{R}^2)\delta^{ij} \right], \quad (8a)$$

$$(\kappa_{DB})^{ij} = \xi \left[-2Q^i R^j + \frac{2}{3}(\vec{Q} \cdot \vec{R})\delta^{ij} \right], \text{ and} \quad (8b)$$

$$(\kappa_{HB})^{ij} = \xi \left[2R^i R^j + \frac{1}{3}(\vec{Q}^2 - \vec{R}^2)\delta^{ij} \right]. \quad (8c)$$

We can see immediately from (8) that the ‘‘linear medium’’ for our electromagnetic fields will be, in general, anisotropic; in fact, the only way for all of these matrices to be isotropic (i.e., proportional to δ^{ij}) is for all of them to vanish, with $\vec{Q} = \vec{R} = 0$.

These κ matrices can also be reparametrized in terms of certain parity-even and parity-odd combinations, denoted $\tilde{\kappa}_{e\pm}$, $\tilde{\kappa}_{o\pm}$, and $\tilde{\kappa}_{\text{tr}}$ [13]; experimental bounds on the components of the tensor $(k_F)^{abcd}$ are usually quoted in terms of these matrices [2]. In our case, we have

$$(\tilde{\kappa}_{e\pm})^{ij} = \xi \left[-Q^i Q^j \pm R^i R^j + \frac{1}{3}(\vec{Q}^2 \mp \vec{R}^2)\delta^{ij} \right], \quad (9a)$$

$$(\tilde{\kappa}_{o+})^{ij} = 2\xi Q^{[i} R^{j]}, \quad (9b)$$

$$(\tilde{\kappa}_{o-})^{ij} = 2\xi \left[-Q^{(i} R^{j)} + \frac{1}{3}(\vec{Q} \cdot \vec{R})\delta^{ij} \right], \text{ and} \quad (9c)$$

$$\tilde{\kappa}_{\text{tr}} = -\frac{\xi}{3}(\vec{Q}^2 + \vec{R}^2). \quad (9d)$$

Since in all of the above expressions a change in the coupling strength ξ is indistinguishable from a simultaneous rescaling of \vec{Q} and \vec{R} , we will define two new vectors $\bar{Q} = \sqrt{|\xi|}\vec{Q}$ and $\bar{R} = \sqrt{|\xi|}\vec{R}$. In terms of these rescaled vectors, we have

$$(\tilde{\kappa}_{e\pm})^{ij} = \bar{\xi} \left[-\bar{Q}^i \bar{Q}^j \pm \bar{R}^i \bar{R}^j + \frac{1}{3}(\bar{Q}^2 \mp \bar{R}^2)\delta^{ij} \right], \quad (10a)$$

$$(\tilde{\kappa}_{o+})^{ij} = 2\bar{\xi}\bar{Q}^{[i}\bar{R}^{j]}, \quad (10b)$$

$$(\tilde{\kappa}_{o-})^{ij} = 2\bar{\xi} \left[-\bar{Q}^{(i}\bar{R}^{j)} + \frac{1}{3}(\bar{Q} \cdot \bar{R})\delta^{ij} \right], \text{ and} \quad (10c)$$

$$\tilde{\kappa}_{\text{tr}} = -\frac{\bar{\xi}}{3}(\bar{Q}^2 + \bar{R}^2), \quad (10d)$$

where $\bar{\xi} = \xi/|\xi| = \pm 1$.

Source	α	δ	$\log_{10} \sigma $
IC 5063	20 ^h 52 ^m 02 ^s	-57°04'08''	-30.8
3A 0557-383	05 ^h 58 ^m 02 ^s	-38°20'04''	-31.2
IRAS 18325-5925	18 ^h 36 ^m 58 ^s	-59°24'08''	-31.0
IRAS 19850-1818	20 ^h 00 ^m 52 ^s	-18°10'27''	-31.0
3C 324	15 ^h 49 ^m 49 ^s	21°25'39''	-32.2
3C 256	11 ^h 20 ^m 43 ^s	23°27'55''	-32.2
3C 356	17 ^h 24 ^m 19 ^s	50°57'40''	-32.2
FIRST J084044.5+363328	08 ^h 40 ^m 45 ^s	36°33'28''	-32.2
FIRST J155633.8+351758	15 ^h 56 ^m 34 ^s	35°17'57''	-32.2
3CR 68.1	02 ^h 32 ^m 29 ^s	34°23'46''	-32.2
QSO J2359-1241	23 ^h 59 ^m 54 ^s	-12°41'48''	-31.1
3C 234	10 ^h 01 ^m 50 ^s	28°47'09''	-31.7
4C 40.36	18 ^h 10 ^m 56 ^s	40°45'24''	-32.2
4C 48.48	19 ^h 33 ^m 05 ^s	48°11'42''	-32.2
IAU 0211-122	02 ^h 14 ^m 17 ^s	-11°58'45''	-32.2
IAU 0828+193	08 ^h 30 ^m 53 ^s	19°13'16''	-32.2

TABLE I. Sources used in the bounds placed in Section III. Bounds on $|\sigma|$ are those from [14]; right ascension α and declination δ were found in the Centre de Données astronomiques de Strasbourg online catalog (<http://cdsweb.u-strasbg.fr/>).

III. CONSTANT-FIELD PARAMETER BOUNDS

In almost all of the literature on Lorentz symmetry violation to date, it is assumed that the Lorentz-violating fields are constant in space, with a possibility of small linearized perturbations about a constant background. The monopole backgrounds that we will be examining are fundamentally non-linear, and so some of the effects we will be examining do not have an analog in the current literature. However, we can still examine the behaviour of our model in the case of a constant background field in order to get an idea of the size of the effects we are looking for.

It is known that if either $\tilde{\kappa}_{e+}$ or $\tilde{\kappa}_{o-}$ is non-zero, electromagnetic waves will experience vacuum birefringence [13, 14]. We can see from the form of (10) that a coupling of the form (4) will always produce birefringence unless both \vec{Q} and \vec{R} are zero. Non-observance of vacuum birefringence will thereby allow us to place stringent bounds on the components \bar{Q}^i and \bar{R}^i , which will in turn allow us to estimate the order of magnitude of the parameter combination $\sqrt{|\xi|}b$. As we shall see, it is this last combination of parameters that will determine the magnitude of the light-bending effects that are the primary concern of this paper.

To do this, we apply the results of the analysis of Kostelecký and Mewes in [14]. Their analysis was able to place bounds on the magnitude of parameter σ (equal to twice the difference in the phase velocity between the two polarizations) for a list of sixteen optical and infrared sources, shown in Table I. This parameter σ_A for a given source A can in turn be expressed in terms of the compo-

nents of the tensor $(k_F)^{abcd}$ and the right ascension and declination of the source $\{\alpha_A, \delta_A\}$. Putting all of these together, then, we see that each independent bound on σ_A will constrain some polynomial function of the \bar{Q}^i and \bar{R}^i , and that this function will depend on the right ascension and declination of the source in question. The actual form of these functions is quite complicated, and the reader is referred to the Appendix for details on how they are constructed.

We treat each of these sixteen two-sided bounds in [14] as a strict exclusion; this leaves a small region of parameter space near the origin that is allowed under the simultaneous imposition of all of the bounds. The maximum magnitudes of the components \bar{Q}^x , \bar{Q}^y , and \bar{Q}^z in this allowed region of parameter space are 1.56×10^{-16} , 1.54×10^{-16} , and 1.43×10^{-16} respectively. The bounds on the magnitudes of \bar{R}^x , \bar{R}^y , and \bar{R}^z are identical; this is to be expected, since all of the coefficients that control birefringent effects (i.e., the components of $\tilde{\kappa}_{e+}$ and $\tilde{\kappa}_{o-}$) are antisymmetric under the exchange $\vec{Q} \leftrightarrow \vec{R}$ and all of our observational bounds are taken to be symmetric about zero. Finally, the value of $\xi B_{ab}B^{ab} = 2\xi(-\vec{Q}^2 + \vec{R}^2)$ in the allowed region of parameter space is bounded by

$$|\xi B_{ab}B^{ab}| < 4.59 \times 10^{-32}. \quad (11)$$

This bound is symmetric about zero for the same reasons that the individual bounds on the components of \vec{Q} and \vec{R} are the same.

During the course of the preparation of this work, another work [15] was published, based on six polarization measurements of gamma-ray bursts. The bounds on certain components of $(k_F)^{abcd}$ derived in this latter work were much more stringent than those from the work [14], by a factor of approximately 10^6 . However, the bounds on the coefficients of $(k_F)^{abcd}$ in both [14] and [15] are derived under the assumption that the light is not ‘‘accidentally’’ emitted in a normal mode, in which case the birefringent effects would be unobservable. Since our parameter space is effectively six-dimensional, and only six sources were used in the derivation of these newer bounds to begin with, the loss of any one of the newer bounds in [15] would still leave a parameter of our model effectively unconstrained. The larger number of data points used in the earlier work [14] leads to more robust constraints, since deletion of one or two data points would not substantially affect the bounds. In principle, a larger set of measurements of the type and precision found in [15] could be subjected to the same analysis, and one would expect that such an analysis would lead to bounds on $\xi B_{ab}B^{ab}$ that were proportionally more stringent.

IV. MONOPOLE LENSING

A. Ordinary & extraordinary waves

In the previous section, we worked under the assumption that the background field B_{ab} was constant in space and time. However, recent work on monopole solutions [10, 11, 16] has shown that there exist static solutions in which the field B_{ab} varies spatially, both in magnitude and direction. In the context of Lorentz-violating electrodynamics, this means that the κ matrices appearing in the constitutive relations (6) vary from point to point. In other words, in the presence of a monopole solution, electromagnetic fields act as though they were in an inhomogeneous, anisotropic, birefringent medium. In particular, the inhomogeneity of the medium implies that light rays travelling near the monopole will be deflected from straight-line paths.

To quantify this effect, we apply a geometric-optics approximation to the modified Maxwell equations (5). Our derivation will roughly follow the technique of Sluijter *et al.* [17] where applicable.³ We choose an ansatz for the electromagnetic fields of the form

$$\vec{E}(t, \vec{x}) = \vec{e}(\vec{x})e^{ik(S(\vec{x})-t)}, \quad (12a)$$

$$\vec{B}(t, \vec{x}) = \vec{b}(\vec{x})e^{ik(S(\vec{x})-t)}. \quad (12b)$$

Plugging these into the modified Maxwell equations, we obtain the equations

$$\vec{\nabla}S \times \vec{h} + \vec{d} = -\frac{1}{ik}\vec{\nabla} \times \vec{h} \quad (13a)$$

$$\vec{d} \cdot \vec{\nabla}S = -\frac{1}{ik}\vec{\nabla} \cdot \vec{d} \quad (13b)$$

$$\vec{b} \cdot \vec{\nabla}S = -\frac{1}{ik}\vec{\nabla} \cdot \vec{b} \quad (13c)$$

$$\vec{\nabla}S \times \vec{e} - \vec{b} = -\frac{1}{ik}\vec{\nabla} \times \vec{e}, \quad (13d)$$

where we have defined

$$\vec{d} = (\mathbf{1} + \kappa_{DE})\vec{e} + \kappa_{DB}\vec{b}, \quad (14)$$

$$\vec{h} = \kappa_{HE}\vec{e} + (\mathbf{1} + \kappa_{HB})\vec{b}. \quad (15)$$

(Recall that the κ 's in these equations are 3×3 matrices acting on the vectors \vec{e} and \vec{b} .) We then apply the standard geometric-optics approximation, and restrict our attention to solutions for which the length scale variation of the vectors \vec{e} , \vec{b} , \vec{d} , and \vec{h} are much less than the length

³ Note that in Sluijter *et al.* [17], the medium of propagation is assumed to be electrically anisotropic but magnetically isotropic. In the present work, however, our ‘‘medium’’ will turn out to be electrically isotropic but magnetically anisotropic. To apply the results of Sluijter *et al.* to our situation, then, we must effectively switch the roles of \vec{E} and \vec{H} .

scale defined by k . In other words,

$$\left\{ \frac{|\vec{\nabla}\vec{e}|}{|\vec{e}|}, \frac{|\vec{\nabla}\vec{b}|}{|\vec{b}|}, \frac{|\vec{\nabla}\vec{d}|}{|\vec{d}|}, \frac{|\vec{\nabla}\vec{h}|}{|\vec{h}|} \right\} \ll k \quad (16)$$

in some appropriate sense, which allows us to neglect the right-hand sides of the four equations (13). Note that if the length-scale of variation of the κ matrices is “small” in this sense, then the slow variation of \vec{d} and \vec{h} follows from the slow variation of \vec{e} and \vec{b} .

So far in this section, we have not assumed that the κ matrices have any particular form; our equations are valid for any (static) background field B_{ab} , assuming it is static and slowly varying. For the case of the monopole solution originally found in [10], the field configuration is of the form

$$B_{\theta\phi} = g(r)r^2 \sin\theta, \quad (17)$$

with all other components vanishing. The function $g(r)$ is the solution to the differential equation⁴

$$\frac{\partial}{\partial r} \left(\frac{\partial g}{\partial r} + \frac{2}{r}g \right) - 2\lambda(2g^2 - b^2)g = 0 \quad (18)$$

subject to the boundary conditions $g(0) = 0$ and $g(\infty) = b/\sqrt{2}$. While a closed-form solution for $g(r)$ is not known, its asymptotic behaviour as $r \rightarrow \infty$ is

$$g(r) = \frac{b}{\sqrt{2}} \left(1 - \frac{1}{4\lambda b^2 r^2} - \frac{3}{8\lambda^2 b^4 r^4} + \dots \right). \quad (19)$$

In terms of the “electric” and “magnetic” vectors \vec{Q} and \vec{R} , it can easily be shown that for this solution we have $\vec{Q} = 0$ and

$$\vec{R} = g(r)\hat{r}. \quad (20)$$

From Equation (8), we see that the “off-diagonal” matrices κ_{DB} and κ_{HE} vanish, and that κ_{DE} becomes isotropic:

$$(\kappa_{DE})^{ij} = -\frac{1}{3}\xi g^2(r)\delta^{ij} \quad (21)$$

$$(\kappa_{HB})^{ij} = \xi g^2(r) \left(2\hat{r}^i \hat{r}^j - \frac{1}{3}\delta^{ij} \right). \quad (22)$$

This allows us to define effective permittivity and permeability tensors ϵ^{ij} and μ^{ij} such that $d^i = \epsilon^{ij}e^j$ and $b^i = \mu^{ij}h^j$. The permittivity tensor will be

$$\epsilon^{ij} = \delta^{ij} + (\kappa_{DE})^{ij} = \left(1 - \frac{1}{3}\xi g^2 \right) \delta^{ij}, \quad (23)$$

while the inverse of the permeability tensor will be

$$(\mu^{-1})^{ij} = \delta^{ij} + (\kappa_{HB})^{ij} = \left(1 - \frac{1}{3}\xi g^2 \right) \delta^{ij} + 2\xi g^2 \hat{r}^i \hat{r}^j. \quad (24)$$

This last matrix can be inverted to yield

$$\mu^{ij} = \frac{1}{1 - \frac{1}{3}\xi g^2} \left[\delta^{ij} - \frac{2\xi g^2}{1 + \frac{5}{3}\xi g^2} \hat{r}^i \hat{r}^j \right]. \quad (25)$$

In the language of birefringent optics, then, the “medium” in which our waves are propagating will be electrically isotropic, magnetically anisotropic, and unaxial; the “optical axis” of the medium will be the radial direction \hat{r} .

Combining all of the above, then, we have from (13a) and (14)

$$\vec{e} = -\frac{1}{\epsilon}(\vec{\nabla}S) \times \vec{h}, \quad (26)$$

where $\epsilon = 1 - \frac{1}{3}\xi g^2$ is the (position-dependent) permittivity. Plugging this in to (13d), and defining the wave-normal vector $\vec{p} = \vec{\nabla}S$, we obtain

$$[p^i p^j - (\vec{p} \cdot \vec{p})\delta^{ij} + \epsilon\mu^{ij}] h^j = 0. \quad (27)$$

For a non-trivial wave amplitude \vec{h} to exist, it must be the case that

$$\det [p^i p^j - p^2 \delta^{ij} + \epsilon\mu^{ij}] = 0; \quad (28)$$

after some algebra, this condition boils down to

$$(p^2 - 1) \left(p^2 - \frac{\zeta}{1 + \zeta} (\vec{p} \cdot \hat{r})^2 - \frac{1}{1 + \zeta} \right) = 0, \quad (29)$$

where

$$\zeta = \frac{2\xi g^2}{1 - \frac{1}{3}\xi g^2}. \quad (30)$$

For a given direction of \hat{r} and value of ζ , the equation (29) defines a surface in \vec{p} -space called the *optical indicatrix*. This surface consists of two ellipsoids which are tangent at the points $\vec{p} = \pm\hat{r}$, and which do not otherwise intersect. These ellipsoids correspond to ordinary and extraordinary waves, respectively; the ordinary waves satisfy

$$\mathcal{H}_o = \frac{1}{2}(p_o^2 - 1) = 0, \quad (31)$$

while the extraordinary waves satisfy

$$\mathcal{H}_e = \frac{1}{2}((1 + \zeta)p_e^2 - \zeta(\vec{p}_e \cdot \hat{r})^2 - 1) = 0. \quad (32)$$

(The reason for the choice of the overall factors in these equations will become clear in Section IV B.)

⁴ This equation is just the equation of motion for B_{ab} derived from the Lagrangian (2), under the imposition of the ansatz (17).

For the ordinary waves, requiring that $\vec{p}_o = \hat{p}_o$ is a unit vector causes Equation (27) to reduce to

$$\left[\hat{p}_o^i \hat{p}_o^j - \frac{\zeta}{1+\zeta} \hat{r}^i \hat{r}^j \right] h_o^j = 0, \quad (33)$$

It is not hard to see that for this to be true, the vector \vec{h}_o must be at right angles to both \hat{p}_o and \hat{r} .⁵ In other words, we can define the magnetic field direction \hat{h}_o as

$$\hat{h}_o = \frac{\hat{p}_o \times \hat{r}}{|\hat{p}_o \times \hat{r}|}. \quad (34)$$

Equation (13a) then tells us that the (electric) polarization of the ordinary wave \hat{e}_o is given by

$$\hat{e}_o = \frac{\hat{r} - \hat{p}_o(\hat{p}_o \cdot \hat{r})}{|\hat{r} - \hat{p}_o(\hat{p}_o \cdot \hat{r})|}. \quad (35)$$

In other words, the electric polarization for an ordinary wave points along the projection of \hat{r} in the plane orthogonal to \hat{p}_o . These waves propagate at constant speed through space, since p_o^2 is constant.

The polarization of the extraordinary waves is somewhat less obvious. We shall simply cite the work of [17]; with the substitution $\vec{E} \leftrightarrow \vec{H}$ (as noted in Footnote 3), the magnetic field direction \hat{h}_e for an extraordinary wave with wave front vector \vec{p}_e can be seen to point in the direction

$$\hat{h}_e = \frac{(\vec{p}_e \times \hat{r}) \times [(1+\zeta)\vec{p}_e - \zeta(\vec{p}_e \cdot \hat{r})\hat{r}]}{|\vec{p}_e \times \hat{r}| \times [(1+\zeta)\vec{p}_e - \zeta(\vec{p}_e \cdot \hat{r})\hat{r}]}, \quad (36)$$

while the electric field vector \hat{e}_e will point in the direction

$$\hat{e}_e = -\frac{\vec{p}_e \times \hat{r}}{|\vec{p}_e \times \hat{r}|}. \quad (37)$$

Note that the magnetic polarization direction \hat{h}_e is not, in general, perpendicular to the extraordinary wave-front vector \vec{p}_e .

B. Ray-tracing

To trace the paths of rays in the presence of a monopole background, we follow the method of Sluijter *et al.* [17] and interpret the factors \mathcal{H}_o and \mathcal{H}_e as point-particle Hamiltonians, whose trajectories evolve with respect to some parameter τ . In other words, we expect that for both ordinary rays and extraordinary rays, their position $\vec{x}(\tau)$ and momentum $\vec{p}(\tau)$ will satisfy

$$\frac{d\vec{x}}{d\tau} = \nabla_{\vec{p}} \mathcal{H} \quad \text{and} \quad \frac{d\vec{p}}{d\tau} = -\nabla_{\vec{x}} \mathcal{H}. \quad (38)$$

⁵ In the case where $\hat{p}_o \parallel \hat{r}$, the wave direction is parallel to the optical axis, and so the ordinary and extraordinary waves travel at the same speed.

Under this interpretation, it is evident that the ordinary rays will travel in straight lines: the ordinary Hamiltonian \mathcal{H}_o is simply that of a free particle, and we will have

$$\frac{d\vec{x}}{dt} = \vec{p} \quad \text{and} \quad \frac{d\vec{p}}{dt} = 0. \quad (39)$$

(The insertion of the extra factors of $\frac{1}{2}$ in Equations (31) and (32) was done to make these equations look “nice”.) Thus, the velocity \vec{v}_o of an ordinary ray is constant with respect to time. Its electric and magnetic polarization directions will also be constant along its path: since the velocity is parallel to the wave-normal direction \hat{p}_o , it can be seen from (34) and (35) that \vec{v}_o , \hat{h}_o , and \hat{e}_o are always mutually orthogonal, with \hat{h}_o perpendicular to the plane containing \vec{v}_o and \hat{r} .

The paths of the extraordinary rays are less straightforward to find. It is illustrative to pass from the Hamiltonian formulation for ray’s motion to a Lagrangian formulation. This can be done by performing a Legendre transformation on \mathcal{H}_e :

$$\mathcal{L}_e(\vec{x}, \dot{\vec{x}}) = \vec{p} \cdot \dot{\vec{x}} - \mathcal{H}_e, \quad (40)$$

where \vec{p} can be written as a function of $\dot{\vec{x}}$ by inverting the relation

$$\dot{\vec{x}} = \nabla_{\vec{p}} \mathcal{H}_e = (1+\zeta)\vec{p}_e - \zeta(\vec{p}_e \cdot \hat{r})\hat{r}. \quad (41)$$

(It can then be seen from (36), (37) and (41) that \vec{v}_e , \hat{h}_e , and \hat{e}_e are mutually orthogonal, as is the case for the ordinary rays.) To perform this Legendre transform, we define an inverse metric tensor g^{ij} as

$$g^{ij} = (1+\zeta)\delta^{ij} - \zeta\hat{r}^i\hat{r}^j, \quad (42)$$

in terms of which we have

$$\mathcal{H}_e = \frac{1}{2} (g^{ij} p_i p_j - 1). \quad (43)$$

(The extra factors of $(1+\zeta)$ in (32) were chosen to make this inverse metric more tractable.) It can then be seen that $\dot{x}^i = g^{ij} p_j$; inverting this, we then have $p_i = g_{ij} \dot{x}^j$, where g_{ij} is the metric tensor itself:

$$g_{ij} = \frac{1}{1+\zeta} \delta_{ij} + \frac{\zeta}{1+\zeta} \hat{r}_i \hat{r}_j. \quad (44)$$

Performing the Legendre transformation on \mathcal{H}_e , then, we find an effective point-particle Lagrangian for the extraordinary rays:

$$\mathcal{L}_e = \frac{1}{2} (g_{ij} \dot{x}^i \dot{x}^j + 1), \quad (45)$$

or, in terms of the path of the particle in spherical coordinates $\{r(\tau), \theta(\tau), \phi(\tau)\}$,

$$\mathcal{L}_e = \frac{1}{2} \left[\dot{r}^2 + \frac{1}{1+\zeta} r^2 (\dot{\theta}^2 + \sin^2 \theta \dot{\phi}^2) + 1 \right]. \quad (46)$$

This Lagrangian is independent of ϕ and t , implying that there are two constants of the motion: the angular momentum in the z -direction, given by

$$\ell = \frac{1}{1+\zeta} r^2 \sin^2 \theta \dot{\phi}, \quad (47)$$

and the “energy,”

$$E = \frac{1}{2} \left[\dot{r}^2 + \frac{1}{1+\zeta} r^2 \left(\dot{\theta}^2 + \sin^2 \theta \dot{\phi}^2 \right) - 1 \right] = 0. \quad (48)$$

Restricting our attention to the equatorial plane ($\theta = \frac{\pi}{2}$), we can write this as

$$\frac{1}{2} \left[\dot{r}^2 + (1+\zeta) \frac{\ell^2}{r^2} - 1 \right] = 0 \quad (49)$$

The motion of an extraordinary ray in the presence of a Lorentz-violating monopole is therefore equivalent to the motion of a particle with unit mass and total energy $E = 0$ in an effective one-dimensional potential

$$V_{\text{eff}}(r) = \frac{\ell^2(1+\zeta)}{2r^2} - \frac{1}{2}. \quad (50)$$

We now wish to calculate the trajectory of a ray originating far from the monopole and passing nearby it. Combining (47) and (49), we can write down a differential equation relating r and ϕ along the trajectory:

$$\frac{d\phi}{dr} = \frac{\dot{\phi}}{\dot{r}} = \pm \frac{\ell(1+\zeta)r^{-2}}{\sqrt{1 - \ell^2(1+\zeta)r^{-2}}}. \quad (51)$$

The total angle of deflection $\Delta\phi$ of the light ray can then in principle be found by integrating (51) from $r = \infty$ to r_{min} (defined as the value of r for which $\dot{r} = 0$ in (49) above) and doubling the result. However, a closed-form analytic expression for $\Delta\phi$ cannot be found, for the simple reason that ζ is a function of r , due to its dependence on the field profile g ; and as noted above, we do not have a closed-form expression for $g(r)$.⁶ We can, however, plug (19) into (30) to obtain a power series for ζ in powers of r^{-1} . Moreover, since ξb^2 is expected to be many orders of magnitude less than one, we can safely discard any terms of $\mathcal{O}(\xi^2 b^4)$ or higher. All told, then, we have the approximation

$$\zeta = \xi b^2 - \frac{\xi b^2}{2\lambda b^2 r^2} + \mathcal{O}(\xi^2 b^4, r^{-4}). \quad (52)$$

Defining $\mu = \xi b^2$ and $\nu = (2\lambda b^2 \ell^2)^{-1}$, and substituting $u = \ell/r$, we can write our integral for $\Delta\phi$ as

$$\Delta\phi \approx \int_0^{u_{\text{max}}} \frac{1 + \mu - \mu\nu u^2}{\sqrt{1 - (1 + \mu)u^2 + \mu\nu u^4}} du \quad (53)$$

⁶ Even if we wanted to evaluate this integral numerically using a numerical solution for the field profile, we would still expect the geometric-optics approximation to break down near the monopole core; in this region, the length scale of the field variation would presumably be shorter than the wavelength of the light waves being deflected.

where $u_{\text{max}} = \ell/r_{\text{min}}$. This quantity can then be evaluated to leading order in μ and ν , either by differentiation with respect to μ and ν or in terms of complete elliptic integrals. To linear order in μ and ν , the result is

$$\Delta\phi \approx \frac{\pi}{2} \left(1 + \frac{\mu}{2} (1 - \nu) \right). \quad (54)$$

The deflection angle α between the propagation direction of the incoming ray and the outgoing ray will then be

$$\alpha = 2\Delta\phi - \pi \approx \frac{\pi}{2} \xi b^2 \left(1 - \frac{1}{2\lambda b^2 \ell^2} \right), \quad (55)$$

where a positive value of α corresponds to a ray being attracted towards the monopole, and a negative value corresponds to a ray being repelled from the monopole. Note that the sign of α is the same as the sign of ξ ; the quantity in parentheses must be assumed to be positive, since the quantity $\nu = (2\lambda b^2 \ell^2)^{-1}$ has been assumed to be small.

It is instructive to ask what the meaning of the parameter ν is in the above calculation. To interpret it, we must assign some meaning to the constant of the motion ℓ ; the most illuminating way to do this is to relate it to the impact parameter β of the ray. The asymptotic velocity of the ray (at $r \rightarrow \infty$) can be seen from (49) to be $\dot{r} = \pm 1$; the plus or minus corresponds to infalling or outgoing rays. It can also be shown geometrically that a particle at location $(x, y_0, 0)$ with velocity $(-v, 0, 0)$ will have $\dot{\phi} = yv/r^2$. Thus, the quantity ℓ defined in (47) will be for this particle

$$\ell = \frac{1}{1+\zeta} y_0 v, \quad (56)$$

In the limit $x \rightarrow \infty$ with y_0 fixed, we can identify y_0 with the impact parameter β for this trajectory; thus,

$$\ell = \frac{1 - \frac{1}{6}\xi b^2}{1 + \frac{5}{6}\xi b^2} \beta, \quad (57)$$

where the prefactor comes from taking the limit of ζ as $r \rightarrow \infty$.

It is important to note that ℓ is not exactly equal to the impact parameter in these units; however, since our result for the angular deflection (55) is only accurate to $\mathcal{O}(\xi^2 b^4)$, we can effectively replace ℓ with the impact parameter in this equation:

$$\alpha = 2\Delta\phi - \pi \approx \frac{\pi}{2} \xi b^2 \left(1 - \frac{1}{2\lambda b^2 \beta^2} \right), \quad (58)$$

Note, meanwhile, that the characteristic length scale of the monopole core (as found in [10]) is $r_M = (\sqrt{\lambda} b)^{-1}$. Thus, we have $\nu = \frac{1}{2}(r_M/\beta)^2$; in other words, ν is best thought of as telling us about the ratio of the physical size of the monopole to the impact parameter of the ray.

V. DISCUSSION

We have shown that a direct coupling between the Maxwell field and an antisymmetric tensor field will, in general, cause birefringent effects. Moreover, these effects are dependent on the local magnitude of the field; this implies that a light ray will be deflected depending on its polarization. Light rays whose electric polarization vector lies in the scattering plane (“ordinary rays”) will travel past the monopole undeflected; those whose electric polarization is perpendicular to the scattering plane, meanwhile (“extraordinary rays”) will be deflected due to their varying speed of light. The leading-order angular deflection of these extraordinary rays, in terms of the model’s parameters ξ , λ , and b and the ray’s impact parameter β is given in (58).

These effects are similar to the gravitational lensing effects derived in previous work on the Lorentz-violating monopole solutions [10, 11, 16], although there are some important differences as well. In the work of Li *et al.* [16], the gravitational deflection of a null ray due to a Lorentz-violating monopole solution is shown to be

$$\alpha_G = \frac{3}{2}\pi\epsilon - \frac{\sqrt{\epsilon}}{\sqrt{\lambda}br_m} + \frac{\epsilon}{20\lambda b^2 r_m^2} + \mathcal{O}(r_m^3), \quad (59)$$

where $\epsilon = 16\pi Gb^2$ and r_m is the radial coordinate of closest approach for the null ray in question. The most notable similarity between the gravitational deflection α_G and the direct-coupling deflection α is that in both cases, the deflection angle does not vanish in the limit of large impact parameter. (This is to be contrasted with the case of light deflection by a conventional Schwarzschild metric, for which the deflection angle goes to zero as the impact parameter gets large.) In our case, we have

$$\alpha_\infty \equiv \lim_{\beta \rightarrow \infty} \alpha = \frac{\pi}{2}\xi b^2; \quad (60)$$

the corresponding quantity in the gravitational case is $(\alpha_G)_\infty = \frac{3}{2}\pi\epsilon$. In this asymptotic limit, light rays behave as though there was a conical deficit angle due to the monopole.

However, this observation also illuminates an important difference between the direct-coupling case and the gravitational case. As noted previously, the coupling parameter ξ can be either positive or negative; from (55), this implies that extraordinary rays are attracted towards the monopole when $\xi > 0$, but are repelled by it when $\xi < 0$. In the limit $\beta \rightarrow \infty$, the light rays behave as if in a space with a conical deficit angle when ξ is positive, and a “conical surplus angle” when ξ is negative. In contrast, light rays are always deflected towards a monopole solution by its gravitational influence, since ϵ (and therefore α_G , in the regime where (59) is valid) is always positive.

We can also ask what we would see if a monopole lay between us and a distant star, in the case where $\xi \neq 0$ but neglecting the gravitational effects on the light rays. For simplicity, consider the case in which the ray trajectory

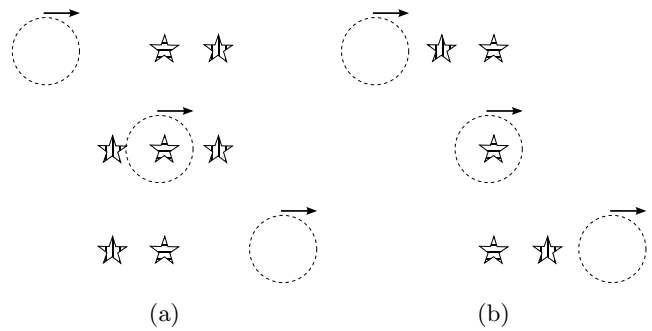


FIG. 1. Multiple images of a distant star created by a passing monopole with (a) $\xi > 0$; (b) $\xi < 0$. The monopole’s location is indicated by the dashed circle; the (electric) polarization of the light from each image is indicated by the direction of its stripes.

stays far from the monopole, and so the approximation $\nu \approx 0$ is valid. It will always be the case that the ordinary rays sent out by the star will reach us along a straight-line path; the image observed this way would be highly polarized, but otherwise undistorted. However, the extraordinary rays would form zero, one, or two images, depending on the sign of ξ and the angular separation between the monopole and the distant star on the sky. A schematic illustration of the images of a distant star created by a passing monopole is shown in Figure 1.

Of particular note is that there is *always* a double image of the star due to the birefringent effects of the monopole; the angular separation of the ordinary image and extraordinary image (in the limit $\nu \rightarrow 0$) will be

$$\theta_E = \frac{\pi}{2}\xi b^2 \frac{D_{MS}}{D_S}, \quad (61)$$

where D_{MS} is the distance to the source from the monopole and D_S is the distance to the star.⁷ Given the non-observation of such double images on the sky, we can immediately say that if ξb^2 is non-zero, it must be sufficiently small that these double images are not observed. If we take the maximum angular resolution of the Very Long Baseline Array (about 1.2×10^{-4} arcseconds [18]) as the best achievable resolution with current technology, we must thereby conclude that $|\xi b^2| < 10^{-10}$ or so. This is, of course, a much less stringent bound than those placed on ξb^2 via direct polarimetry measurements (see Section III); we therefore conclude that these multiple images will, in general, be so closely spaced as to be unresolvable. However, the effects of this coupling would still in principle be observable via intensity variations of the starlight, either due to the appearance and disappearance of the aforementioned multiple images, or via

⁷ The angle θ_E would also be the radius of the “Einstein ring” in the case of perfect alignment between Earth, the monopole, and the distant star.

more conventional microlensing effects. We are currently investigating these possibilities.

Finally, we note that the coupling (4) is not the only possible coupling between an antisymmetric tensor field B_{ab} and the Maxwell field A_a . In particular, one could also couple B_{ab} to the Maxwell field by postulating an “effective metric” $\tilde{\eta}^{ab}$, differing from the “canonical” metric η^{ab} :

$$\tilde{\eta}^{ab} = \eta^{ab} + \chi B^a{}_c B^{bc} \quad (62)$$

The Lagrangian for a Maxwell field that operates under this metric instead of η^{ab} would then be

$$\mathcal{L} = -\frac{1}{4} \tilde{\eta}^{ac} \tilde{\eta}^{bd} F_{ab} F_{cd} = -\frac{1}{4} \left(F_{ab} F^{cd} + (\tilde{k}_F)^{abcd} F_{ab} F_{cd} \right), \quad (63)$$

where

$$(\tilde{k}_F)^{abcd} = \frac{\chi}{2} \left[B^{[a}{}_{e} \eta^{b][c} B^{d]e} + \frac{2}{3} \eta^{a[c} \eta^{d]b} B_{ef} B^{ef} \right] + \mathcal{O}(\chi^2 b^4). \quad (64)$$

The effects of this coupling could presumably be analysed using the same methods in this work. Importantly, however, this coupling should not lead to birefringent effects (for the same reasons that the “generalized bumblebee models” analysed in [7] did not lead to birefringence.) The parameter χ in such a model would therefore evade the stringent constraints that were imposed by polarimetry on the parameter χ in our original coupling (4).

ACKNOWLEDGMENTS

We thank Matthew Mewes and Brett Altschul for helpful discussions during the preparation of this work.

Appendix: Dependence of σ on model parameters

Following the language of [13], the parameter σ for a source with right ascension α and declination δ is given

by

$$\sigma^2 = (\vec{\zeta}_a \cdot \vec{k})^2 + (\vec{\zeta}_c \cdot \vec{k})^2, \quad (A.1)$$

where we have defined the three ten-dimensional vectors in this equation as

$$\zeta_s^a = \begin{bmatrix} \cos^2 \delta + \cos^2 \alpha - \sin^2 \alpha \sin^2 \delta \\ \sin^2 \delta \cos^2 \alpha - \cos^2 \delta - \sin^2 \alpha \\ -2 \sin \delta \sin \alpha \cos \alpha \\ -\sin \delta \sin \alpha \cos \alpha \\ \sin \delta (\sin^2 \alpha - \cos^2 \alpha) \\ -\cos \delta \sin \alpha \\ \cos \delta \cos \alpha \\ -\sin \delta \cos \delta \cos \alpha \\ -\cos^2 \delta \sin \alpha \cos \alpha \\ -\sin \delta \cos \delta \sin \alpha \\ -2 \sin \delta \sin \alpha \cos \alpha \\ -2 \sin \delta \sin \alpha \cos \alpha \end{bmatrix}, \quad (A.2)$$

$$\zeta_c^a = \begin{bmatrix} \frac{1}{2}(1 + \sin^2 \delta)(\sin^2 \alpha - \cos^2 \alpha) \\ \frac{1}{2}(\sin \delta + \sin^2 \alpha - \sin^2 \delta \cos^2 \alpha) \\ (1 + \sin^2 \delta) \sin \alpha \cos \alpha \\ -\sin \delta \cos \delta \cos \alpha \\ -\sin \delta \cos \delta \sin \alpha \\ \cos \delta \sin \alpha \\ \sin \delta (\sin^2 \alpha - \cos^2 \alpha) \\ -\cos \delta \cos \alpha \end{bmatrix}, \quad (A.3)$$

and

$$k^a = \begin{bmatrix} -\bar{Q}^y \bar{R}^y + \frac{1}{3} \bar{Q} \cdot \bar{R} \\ \bar{Q}^x \bar{R}^x - \frac{1}{3} \bar{Q} \cdot \bar{R} \\ (\bar{Q}^y)^2 - (\bar{R}^y)^2 - \frac{1}{3} (\bar{Q}^2 - \bar{R}^2) \\ (\bar{Q}^z)^2 - (\bar{R}^z)^2 - \frac{1}{3} (\bar{Q}^2 - \bar{R}^2) \\ \bar{Q}^x \bar{Q}^y - \bar{R}^x \bar{R}^y \\ \bar{Q}^x \bar{Q}^z - \bar{R}^x \bar{R}^z \\ \bar{Q}^y \bar{Q}^z - \bar{R}^y \bar{R}^z \\ \bar{Q}^x \bar{R}^z + \bar{Q}^z \bar{R}^x \\ -\bar{Q}^x \bar{R}^y - \bar{Q}^y \bar{R}^x \\ \bar{Q}^y \bar{R}^z + \bar{Q}^z \bar{R}^y \end{bmatrix}. \quad (A.4)$$

Note that this last vector contains the ten independent parameters of the matrices $\tilde{\kappa}_{e+}$ and $\tilde{\kappa}_{o-}$.

[1] Colladay, D. and Kostelecký, V. A., Physical Review D, **58**, 116002 (1998).
 [2] Kostelecký, V. A. and Russell, N., “Data Tables for Lorentz and CPT Violation.” (2008), ArXiv:0801.0287v6.
 [3] Kostelecký, V. A., Physical Review D, **69**, 105009 (2004).

[4] Bluhm, R. and Kostelecký, V. A., Physical Review D, **71**, 065008 (2005).
 [5] Bluhm, R., Fung, S.-H., and Kostelecký, V. A., Physical Review D, **77**, 065020 (2008).
 [6] Seifert, M. D., Physical Review D, **79**, 124012 (2009).
 [7] Seifert, M. D., Physical Review D, **81**, 065010 (2010).

- [8] Kostelecký, V. A. and Potting, R., *Physical Review D*, **79**, 065018 (2009).
- [9] Altschul, B., Bailey, Q. G., and Kostelecký, V. A., *Physical Review D*, **81**, 065028 (2010).
- [10] Seifert, M. D., *Physical Review Letters*, **105**, 201601 (2010).
- [11] Seifert, M. D., *Physical Review D*, **82**, 125015 (2010).
- [12] Kibble, T., *Journal of Physics A: Mathematical and General*, **9**, 1387 (1976).
- [13] Kostelecký, V. A. and Mewes, M., *Physical Review D*, **66**, 056005 (2002).
- [14] Kostelecký, V. A. and Mewes, M., *Physical Review Letters*, **87**, 251304 (2001).
- [15] Kostelecký, V. A. and Mewes, M., *Physical Review Letters*, **110**, 201601 (2013).
- [16] Li, X.-Z., Xi, P., and Zhang, Q., *Physical Review D*, **85**, 085030 (2012).
- [17] Sluijter, M., de Boer, D. K. G., and Braat, J. J. M., *Journal of the Optical Society of America. A, Optics, image science, and vision*, **25**, 1260 (2008).
- [18] National Radio Astronomy Observatory, *VLBA Observational Status Summary 2013B* (2013), available at science.nrao.edu/facilities/vlba/docs/.